Simplified Material Model for Concrete Containing High-Content of Tire-Derived Coarse Aggregate under Compression Loading

Abdelmoneim El Naggar, Hany El Naggar, and Pedram Sadeghian

Department of Civil and Resource Engineering, Dalhousie University, 1360 Barrington Street, Halifax, NS, B3H 4R2 Canada

ABSTRACT

The flexible properties of the shredded rubber tires give rubberized concrete desirable properties such as lower relative density, and better dampening ability, higher toughness, and improved deformability resulting in an enhanced dynamic performance. Limited work has been done in modeling these effects. In this study, natural coarse aggregates in concrete mixes were replaced by volume by shredded tires up to 100% replacement ratios following 10% increments. Compression tests were conducted to investigate the effects shredded tires on the mechanical properties of concrete. As expected, the results showed a decrease in the compressive strength and the elastic modulus of the concrete as the replacement ratio increase. Due to compatibility, strain at peak values increased and the integrity of the concrete after failure was enhanced. Models describing the effects shredded tires have on the mechanical properties of the concrete were developed and validated against experimental data from various researchers.

Keywords: Tire Derived Aggregates, Concrete, Modulus, Strength, Strain

DOI: https://doi.org/10.1139/cjce-2019-0626

1. INTRODUCTION

As human dependence and demand on cars and vehicles rise, tire consumption becomes an inevitable problem. This dilemma only spreads with time to pose serious threats to many ecosystems around the world. Every year more than 350 million scrap tires are generated in the US and Canada, with more than 3 billion tires already stockpiled (Wong et al. 2009 and El Naggar et al. 2016). Hence, it comes to no surprise that tire disposal is becoming a worldwide problem. Consequently, more useful and harmless disposal methods must be adopted to tackle the many rising tire stockpiling problems facing our environment. Concrete is second only to water as the most widely used material, with 3 tonnes per year used per capita on average (Gagg 2014). Hence, by incorporating shredded tires into the concrete matrix, a major environmental dilemma could be effectively solved, and at the same time, infrastructure would benefit from the new properties arising from such a unique combination.

Tire derived aggregates (TDA), which is basically shredded tires, have many unique properties that could make it useful in many civil engineering applications (Sparkes et al. 2019). For example, El Naggar et al. (2013) and Mahgoub and Elnaggar (2019, 2020a, and 2020b) illustrated that using a layer of TDA backfill around or above buried pipes is an excellent construction alternative to enhance the stress bridging mechanism and reduce the demand on the pipes. Likewise, TDA excellent seismic properties coupled with its relative lightweight and durability could allow it to make concrete based structures tougher, more ductile and ultimately a better seismic performer. Gravel based concrete is usually brittle and has a relatively high compressive strength but lower tensile strengths. However, great compressive strengths are not always sought after in certain designs. TDA could provide the desired balance between strength and durability for structures experiencing constant dynamic loading that may cause the ordinally

concrete to perform poorly. In seismic conditions, the TDA would improve the structure's deformability and elasticity. This would prevent tensile cracks and increase the longevity of the structure. Likewise, TDA-concrete mixes could make efficient traffic barriers.

Several research projects have been conducted on rubberizing concrete throughout the last two decades. It has been observed that the compressive strength, modulus of elasticity, splitting tensile strength, and the static flexural strength decrease as the rubber content increases. However, higher rubber content within the concrete matrix improves the ductility and material toughness, due to its increased ability to absorb energy and impact. Siddiqi et al. (2013) investigated the effects of replacing up to 40%, with 10 % increments, of the fine aggregate with rubber crumbs. After 28 days, they found out that the compressive strength decreased by 55% by the 40% replacement of sand by volume for normal rubberized concrete. It was concluded that up to 30% rubberized concrete could be effectively used for structural purposes, as it still had a compressive strength greater than 30 MPa. Recently, Moustafa and ElGawady (2015) and Bandarage and Sadeghian (2019) partially replaced fine aggregates with long shredded rubber particles and found that by increasing the rubber content, the failure patterns of concrete from typical diagonal cracks in compression was changed to a combination of longitudinal and transverse cracks.

On the other hand, Ghally and Cahill (2004) studied the effect of fine rubber particles to partially replaced sand (up to 15% by volume of concrete mixture) and studied the correlation of strength, rubber content, and water to cement ratio in rubberized concrete. Likewise, Pham et al. (2019) concluded that rubberized concrete thus can be used for structural components with sufficient strength and adequate service life up to 15% rubber content. Eldin and Senouci (1992) has also observed the ability of rubberized concrete to absorb a large amount of plastic energy under compression and tension. The same trend in behaviour was found to hold in this study as

discussed later in the paper. This proved that rubberized TDA would be useful for applications requiring great impact resistance. Likewise, Zheng et al. (2008) studied rubberized concretes designed by replacing coarse aggregate in normal concrete with ground and crushed scrap tire rubber by volume ratios. Their study showed that the crushed rubber resulted in a greater reduction in many mechanical properties of the concrete, like its compressive strength and the static and dynamic modulus of elasticity than rubber crumbs. An increase in rubber content increases the concrete elastic deformation capacity. Increasing rubber content decreases the peak and residual axial stresses but increases the peak and residual axial strains. Similarly, the dilation rate of concrete increases, as the lateral strain of the concrete for a given axial strain increases (Gholampour et al. 2017).

Xue and Shinozuka (2013) conducted seismic shaking tests on rubberized concrete cylinders and demonstrated that adding rubber crumb can reduce the seismic force on concrete structures due to the increased damping. This study highlighted that rubberized concrete holds a great potential for improving seismic performance by taking advantage of its enhanced energy dissipation capability. Likewise, Lui et al. (2020) conducted a set of static and dynamic tests and finite element modelling on normal concrete claddings and rubberized concrete claddings. It was determined that the loss factor of the given concrete member increases energy as its rubber content increases, which makes rubberized concrete cladding more suitable for protecting structures that require high energy dissipation capacity, like bridge piers. Tehrani and Miller (2017) investigated concrete specimens containing rubber replacement ratios from 0% to 100% by volume of a lightweight expanded-shale coarse aggregate. After conducting an impact test on the specimens using a falling weight, it was concluded that the tire-derived aggregates reduce the mechanical strength of specimens but enhances ductility and toughness of materials. It was observed that for

rubberized normal-weight aggregate concrete, a non-linear but consistent decrease in compression strength as rubber content increases. As TDA content increased, peak strength decreased but the failure became more gradual and it took a longer time for the crack to advance throughout the specimen.

Siringi (2012) conducted compressive and splitting tensile strength tests on concrete that has 7.5 and 15% of the coarse and fine aggregates replaced by rubber particles and mitigated the reduction in compressive strength by the addition of silica fume and utilization of smaller sized TDA. From the results, it was observed that 7-10% of weight of mineral aggregates can be replaced by an equal volume of TDA to produce concrete with compressive strength of up to 27.5 MPa. This rubberized concrete would have higher ductility and toughness with better damage tolerance but the Elastic Modulus would be reduced. Khaloo et al. (2008) found that the maximum toughness index, indicating the post failure strength of concrete, occurs in concretes with 25% rubber content. Li et al. (2014) and Aslani (2015) explored the effect of rubber types and rubber content on mechanical properties of concrete. Accordingaly, constitutive models describing the effect rubber particles have on the concrete mechanical properties were developed. A major limitation for these models is its inability to predict the response for higher rubber volume concrete mixes. The decrease in strength observed by researchers could arise from the fact that replacing coarse aggregate with softer rubber particles results in a clear reduction in the heavy load carrying material (i.e., coarse aggregate), decreasing the overall matrix's carrying capacity. Likewise, the bonding between rubber particles and mortar is usually weaker than the bonding between the original aggregates decreasing the compressive strength (Bideci et al. 2017 and Siddiqi et al. 2013). Finally, the stress concentrations in the paste at the boundaries of the rubber aggregate contributes also to the strength reduction (Zheng et al. 2008).

So far, most research efforts targeting rubberized concrete did not directly target realistic application methods. Most of the studies were conducted using small shredded tires and crumbs. Also, they removed the wires withion the TDA particles, depriving tires from their non-rubber constituents (Tehrani and Miller 2017; Gholampour et al. 2017; Ozbay et al. 2011; Wong et al. 2009; and Biligiri et al. 2018). Shredding the tires to small sizes would be expensive and inefficient, as it would require more energy (El Naggar et al. 2016 and Zahran and El Naggar 2020). A research studying more realistic applications of TDA is needed. Furthermore, constitutive relations that model the performance of rubberized concrete is nonexistent. To be used efficiently, TDA must be refined with the least amount of energy possible, without extensive shredding or separation efforts. Realistic TDA samples must be considered and the combined effects on the concrete matrices must be studied, and constitutive relations must be derived.

Hence, the current research targets replacing coarse aggregate with TDA by volume. Larger TDA particles were included within the concrete matrix, unlike most research efforts studying the effects of substituting fine aggregate with ground rubber. Forty-four specimens were developed and tested under uniaxial compression, after 28 days of curing. 0% to 100% coarse aggregate by volume replacement ratios were used with 10% increments. The specific mechanical properties of the concrete matrices, like compressive strength and strain at peak, along with the modulus of elasticity would be closely studied to determine the performance and effects these concrete mixes with respect to the various infrastructure applications. The derived relationships between TDA content and the various concrete properties (compressive strength, strain at peak, modulus of elasticity, and relative density) would allow the determination of the optimum rubber content. In addition, a constitutive equation describing the stress-strain relationship of rubberized concrete was developed.

2. EXPERIMENTAL PROGRAM

2.1. Test Matrix

A total of 44 concrete cylinders (150 mm x 300 mm) were created including 4 cylinders with ordinary concrete used as control specimens, and 4 specimens for each TDA concentration starting from TDA-10 (10% TDA) up to TDA-100 using 10% increments as indicated in Table 1. The TDA replaced the coarse aggregates by volume, so TDA-10 means that 10% of the coarse aggregate was replaced by TDA and TDA-100 means that the 100% if the coarse aggregate was replaced by TDA. The specimens underwent compressive tests as per ASTM C39 using a 2000 kN hydraulic loading frame to investigate the changes in the mechanical properties of the cylinders containing the TDA, compared to the ordinary concrete cylinders.

2.2. Material Properties

The specimens were constructed using locally sourced material, from batching and recycling facilities. Any TDA particle larger than 19.05 mm was either removed or cut to satisfy the 19.05 mm maximum aggregate size. Sieve analysis was conducted on the different components of the concrete matrix, following ASTM C-136, to gain a better understanding of the gradation of the gravel's individual constituents. The sample size and material specific properties pertaining to each aggregate analyzed are shown in Table 2. The material was placed in the stacked sieves and vibrated in the vibrator for 5 minutes to ensure that the material passage was complete. The sieve analysis was done manually without any sieve vibrators for TDA, however, to ensure that the material passage is accurate. The gradation curves for the used aggregates are shown in Figure 1. Similarly, the bulk densities (shown in Table 2) of the fine aggregates, coarse aggregates, and TDA was obtained using the standard Proctor test (ASTM C29). After filling every third of the

cylindrical container used, the new layer was evenly compacted using 25 strokes with the standard tamping rod, and the material weight and volume was obtained to find the bulk density.

2.3. Specimen Preparation

The concrete matrix used to create the 44 cylinders was found using the Portland Cement Association method, and coarse aggregate was substituted by TDA using volumetric ratios. The general mix design for each TDA content is shown in Table 1. The coarse aggregate, TDA, fine aggregate, cement, and water are added to the mixer accordingly and left to mix for at least 5 minutes to ensure the that the concrete matrix is thoroughly mixed. After mixing, a slump test is carried out following the ASTM C143 to see whether the desired slump (100 mm) was obtained or not. If the slump is less than 100 mm than more superplasticizer is added, and the concrete is mixed again until the 100 mm slump requirement is reached. The mixed concrete is then taken and poured into the cylindrical molds (150 mm x 300 mm). After each third of the cylindrical molds was filled, the concrete was evenly stroked using a tamping rod to ensure that no excessive air pockets exist within the mixture. The concrete is then left to dry in the cylindrical molds for at least 24 hours, then removed from the molds and placed in the curing room for the next 28 days. After 28 days, they are ready for testing. To ensure that the loading surface is flat and even, the two ends of the cylinders are capped by placing them on melted sulfuric compounds and leaving it to harden. Regular flat capping is important to ensure that the testing results would be accurate. An illustration of the preparation process is shown in Figure 2.

2.4. Test Setup and Instrumentation

The uniaxial compression test was conducted using a 2 MN Instron machine using position control approach. The capped cylinders had to be centered along the compressive arms to obtain accurate results. The moving plates applied the compressive loading on the specimens at a rate of 0.5

mm/min based on a preliminary testing of concrete cylinders. The displacement-controled loading approach was selected to capture the post-peak behavior of the specimens. Four linear potentiometers (LPs) were placed to record the displacements resulting from the compressive loading (see Figure 2g). LP#1 and LP#4 were placed off the surface of the cylinder at mid-height facing each other to obtain lateral strain, however the way the LPs were places did not work properly. The data from the horizontal LPs was inconclusive and was not included in this paper. A proper yoke should be used for lateral displacements in the future. LP#2 and LP#3 recorded the vertical displacements and were placed along two steel rings, on the cylinder's middle region, each ring 76.2 mm away the base. The data gained from these potentiometers was used to calculate the axial strain. This information, along with the critical loading, makes the determination of the specimen's mechanical properties possible.

3. RESULTS AND DISCUSSIONS

3.1. Failure Modes

Due to the nature of the compressive tests the specimens underwent, the concrete specimens were only subjected to compressive stress, and hence experienced a compressive failure. The concrete specimens failed at shear mode. Larger macrocracks were qualitatively observed on ordinary concrete and concrete specimens with lower amounts of TDA in them, while thinner microcracks developed on the concrete specimens containing greater amounts of TDA (TDA-30 and above) as can be seen in Figure 3. The microcracks developed towards the cylindrical edge of the specimens and then continued towards the center of the cylinder. Likewise, a greater percentage of TDA in the concrete specimens caused a greater strain at the specimen's peak compressive stress as shown in Figure 4. This greater dilation of the specimen would act as an indicator of failure, preventing the unwanted sudden brittle failure ordinary concrete experiences. This would be very beneficial

for circumstances where early determination that the limit states for a structure are exceeded is key for failure prevention. Likewise, as TDA content increased within the specimens, the failure cracks resulting from the compressive stress become smaller, unlike the ordinary concrete in which the cracks split the specimens and shattered them into pieces some cases. This shows that increasing the TDA content within concrete gives the concrete more ductile properties and flexibility when dealing with certain loads. In other words, increasing the TDA content within a concrete specimen increased the specimen's ability to absorb more energy. Unlike ordinary concrete, TDA content increases the overall integrity of the cylinder, as the specimen remains entact after failure, unlike ordinary concrete and lower TDA content concrete, which ruptured more violently after failure. Hence, adding TDA to allows the concrete to develop gentler and more uniform crack patterns, which is very useful for seismic applications.

3.2. Stress-Strain Behavior

The stress-strain curves depicted in Figure 4 clearly demonstrate how the strain increases as TDA content within the concrete cylinder increases for a given stress value. An enhanced ductile relationship is exhibited within the stress strain curves as the TDA content increases. In a brittle stress-strain relationship, rupture violently occurs without warning. As TDA content increases, a noticeable change in the rate of elongation of the specimen under stress becomes evident as shown in the figure.

The increased strain at peak stress could serve as an indicator for potential failure. This greater strain value might be due to the weak interface between the TDA particles and the other aggregates within the concrete cylinder. This weaker interface results in a more uniform and progressive development of microcracks, which results in a greater increasing rate for the strain values. Furthermore, it is evident that as the TDA content increased the flat segment in the post

failure part of the stress strain curve is longer, which indicates that the concrete toughness is increased.

The increase in strain values at failure stresses as TDA content increased followed a quadratic trendline fashion, as shown in Figure 5a. Each bar represents the average strain at peak stress for the four specimens tested at each TDA content increment, while the error bars shown represent one standard deviation from the mean value. The relatively small error bars indicate a low variability between the results of the tests. Using regression analysis, the normalized strain values can be described by the following equation:

$$\frac{\varepsilon_c}{\varepsilon_{co}} = 2.11 - 4 \times 10^{-5}(R_c - 168)^2 \quad (1)$$

where ε_c is the strain value at peak stress for a given specimen, ε_{co} is the strain at the maximum stress of the ordinary concrete, and R_C is the TDA content (in percent). The average accuracy of the predictions of equation 1 are within less than 4% as can be seen in Figure 5a. The greater deformation experienced at peak stress while still maintaining the overall structural integrity of the specimen holds a significant potential for many applications associated with seismic and dynamic loadings.

3.3. Effect of TDA on Concrete Strength

Compressive Strength Vs. TDA content is plotted in Figure 5b. Each bar represents the average compressive strength of the four identical specimens tested, while the error bars show one standard deviation from the average. The standard deviation varies from 0.61MPa to 1.76 MPa, a small error window, which indicates a low variability of the test results. A 28.63% decrease in compressive strength is experienced in TDA-10 compared to TDA-0 (ordinary concrete). TDA-20's compressive strength decreased by 6.88% compared to TDA-10, which is a 33.55% decrease relative to TDA-0. As the TDA content within a concrete cylinder increased, the concrete's overall

compressive strength decreased as shown in the figure. The percent difference between TDA-100 (100% TDA replacing coarse aggregates) and ordinary concrete strength was 78%. As the TDA content increased, the strength reduction rate decreased until it reached a relatively stable constant near the end. In fact, TDA content and compressive strength almost follow an inverse relationship, specified by:

$$\frac{f'_c}{f'_{co}} = e^{-0.015\,R_c} \qquad (2)$$

where f'_c is the compressive strength of the specimen, f'_{co} is the compressive strength of ordinary concrete (without any TDA) and R_C is the TDA content within the specimen (in percent). As shown in Figure 5b, the equation is a great fit for the observed behavior between the compressive strength and TDA content as the average accuracy of the predictions are within less than 2% of the measured value.

The decrease in compressive strength is a result of the lower modulus of elasticity of TDA and the increased air entrainment which would have allowed premature cracking to occur in the concrete specimens. Likewise, TDA particles do not bond to the other aggregates as strong as ordinary gravel does, so the weak bonding between the TDA particles and the cement paste could have contributed to this lower compressive strength. The concrete specimens experienced less of a brittle failure as TDA content increased, exhibiting more ductile like behaviour and better ability to absorb plastic energy than that of ordinary concrete. Hence, higher TDA content concrete can be used for applications that do not require high compressive strengths but require more a mitigating failure behaviour.

3.4. Energy Adsorption

Energy absorption is an important feature of rubberized concrete under compressive stresses. The amount of energy absorbed by a structural member is obtained by evaluating the integral of the

force-deformation curve of that member multipled by its volume. This was calculated using the trapezoid integral calculation method, where:

$$Total\ Energy\ Adsorption = \sum 0.5(Load_i + Load_{i+1})(Strain_{i+1} - Strain_i) \quad (3)$$

Due to the large deformations of rubberized concrete, especially with higher TDA contents, even though the maximum compressive strength is lower than normal concrete, the amount of energy absorbed is significantly higher as shown in Figure 5c. The specimen with a TDA content of 40% has a roughly 50% higher energy absorption than the control specimen. Whereas the specimen with a 70% TDA content has an approximately 115% higher energy absorption than the control specimen. The relationship between TDA content and energy adsorption can be described by:

$$\frac{E_A}{E_{AO}} = 1.095e^{0.009R_c} \quad (4)$$

Where E_A is the total energy adsorped by the given concrete specimen, R_c is the TDA content (in percent), and E_{AO} is the energy adsorped by the ordinary concrete (without TDA). A relatively exponential fashion is observed in Figure 5c. The average accuracy of the predictions of the obtained relation are within less than 2% of the measured values. The increasing trend between TDA content and energy adsorption explains the enhanced specimen integrity after failure and the better mitigating failure behaviour.

3.5. Effect of TDA on Relative Density

A desirable property that arises from the mixing of TDA with concrete would be the lower concrete density that arises from the lightweight of the shredded tires. This lower weight concrete would be more diserable than an ordinary concrete with the same compressive strength, as the lower stiffness of the structural elements utilizing TDA would allow the stiffer elements to attract more load. This would reduce the dead load demand on the given structural element, which could be highly advantageous in high rise buildings and other large projects that need certain load

distributions to ensure an enhanced behaviour of the overall structure. It is highly disearable to obtain the required concrete strength at the lowest density possible. This unique property combination would be easily obtained using TDA-concrete mixtures. Figure 5d shows the effect of TDA on concrete relative density. Each bar represents the average of four concrete specimens, and the error bars represent one standard deviation away from the mean value. There is a low variability in the relative densities obtained. A relatively constatnt and gradual reduction rate is observed. In fact, the relationship between relative density and TDA content can be described by:

$$\rho = -5.3006R_c + \rho_o \quad (5)$$

where ρ is the concrete relative density, R_c is the TDA content (in percent), and ρ_o is the relative density of the ordinary concrete (without TDA). The variation of relative density with respect to TDA content is shown in Figure 5d. Equation 5 han an average accuracy of the predictions of of less than 1%. Understanding the impact TDA content has on relative density and compressive strength would make the application of rubberized concrete more practical in the engineering field. The equations derived to describe these relations could be of significant help to practicing engineers who desire to create an optimized concrete mix

3.6. Effect of TDA on Concrete Elastic Modulus

Figure 5e shows the variance of concrete elastic modulus with respect to TDA content. Each bar represents the average of the elastic modulus of the four specimens tested for each TDA content increment. The standard deviation bars shown on the graph indicate that the results were of low variance. The elastic modulus was found by calculating the slope corresponding to the relatively linear trend line of stress-strain curve up to 45 percent of compressive strength (f'c). As TDA content increases, the elastic modulus decreases following an exponential fashion given by:

$$\frac{E}{E_o} = \frac{(R_c - 770)^2}{200000} - 1.95 \quad (6)$$

where E represents the elastic modulus at a given TDA content, E_o represents the elastic modulus of the ordinary concrete and R_c represents the TDA content in the concrete specimen (in percent). This decrease in elastic modulus means that the concrete specimen has a lower resistance to be deformed elastically (the specimen has a lower stiffness). As shown in Figure 5e, the replacement of 10% coarse aggregate with TDA (by volume) results in an 8.1% decrease in the elastic modulus with respect to the control ordinary concrete specimens. The elastic modulus continued to experience relatively gradual decreasing rates, until 100% of the coarse aggregates were replaced by TDA, which was followed by a 70% decrease in the elastic modulus with respect to the ordinary control concrete specimen. The elastic modulus decreased by rates varying from 8.1 % to 19.1% with each 10% TDA content increment.

Another model describing the relationship between the elastic modulus and TDA content was developed following the ACI conventional modulus of elasticity equation for normal equation,

$$E = 4700\sqrt{f'_c} \text{ (ACI 318-19)} \quad (7)$$

Since we found that the relationship between the elastic modulus and TDA content is given by equation 4, the ACI equation can be modified to account for the effects of TDA. This modified equation would be :

$$E = [0.0235(R_c - 770)^2 - 9165]\sqrt{f'_{co}} \quad (8)$$

where E represents the elastic modulus, R_c represents the TDA content (in percent), and f'_{co} represents the compressive strength of the ordinary concrete (without TDA). The model is plotted in Figure 5f shown. The developed model accurately fits the data obtained from the lab, which gives the model great application potentials.

3.7. Rubberized Concrete Stress-Strain Model

Understanding the compressive behaviour of rubberized concrete is vital and connot be underestimated. In 1987, using Hognestad's (1951) stress strain model, Mitchell and Collins found a relationship describing the behaviour of regular concrete under compressive strength, which was:

$$f_c = f'_c \left[2.0\left(\frac{\varepsilon_c}{\varepsilon_{oc}}\right) - \left(\frac{\varepsilon_c}{\varepsilon_{oc}}\right)^2\right] \quad (9)$$

where f_c is the concrete compressive strength, f'_c is the concrete strength, ε_c is the concrete strain, and ε_{oc} is the concrete strain at maximum stress. With the relationships derived from the experimental results obtained from the uniaxial compressive tests, the stress strain behaviour of rubberized concrete at a given strength was effectively anticipated. Since the compressive strength of rubberized concrete can be described by equation 2 and the strain behaviour can be modeled by equation 1, then the model describing the behviour of rubberized concrete at a given strength based on the Mitchell and Collins (1987) model would be:

$$f_c = f'_{co}(e^{-0.015\,R_c})\left[\frac{2}{\varepsilon_{oc}}\left(\frac{\varepsilon_c}{2.11-4\times10^{-5}(R_c-168)^2}\right) - \left(\frac{\varepsilon_c/\varepsilon_{oc}}{2.11-4\times10^{-5}(R_c-168)^2}\right)^2\right] \quad (10)$$

where f_c is the concrete compressive strength at given strain ε_c, ε_{oc} is the strain at the maximum stress of the ordinary concrete (without TDA), f'_{co} is the compressive strength of the ordinary concrete, and R_C is the TDA content (in percent).

4. MODEL VALIDATION

The developed rubberized concrete stress strain model was validated against stress strain results from this study and other experminental studies to asses the accuracy of the developed model. The model agrees significantly with the test results of this study as shown in Figure 6 for rubberized concrete with 20%, 40%, and 80% TDA. Abyenah et al. (2018) evaluated the effect of TDA

percentage on the mechanical properties of concrete specimens. 12 cylindrical concrete specimens with the dimensions of 150×300 mm was prepared, with rubber content ranging from 0%-15% via 5% increments. The specimens were tested under uniaxial compression up to failure. The fine and coarse aggregates were acquired in saturated surface dry (SSD) condition. The TDA size used ranged from 12.7-25.4 mm. the fine aggregates ranged in size from 0.075 to 4.75 mm, whereas the coarse aggregates ranged from 0.6 to 16 mm. The 28-day compressive strength of the ordinary concrete prepared was around 63 MPa, while the strain at peak is 0.0027 mm. the stress strain curves can be seen in Figure 7, which are flow in great agreement with the proposed stress-strain model.

Siringi (2012) experimented with TDA particles ranging from 4.75 mm to 50.8 mm in size. He used these rubber particles to replace the coarse aggregates in concrete. The coarse aggregate maximum size was 37.5 mm, and the cement used was high strength Portland cement. Several 150 mm by 300 mm concrete cylinders were made using different amounts of TDA and tested for compressive strength in order to establish the maximum amount of TDA that can be used to replace coarse aggregates without significantly compromising the strength of concrete. Likewise, the same procedure was followed with crumb rubber which replaced the fine aggregates in the concrete with an equal volume of crumb rubber, to study the effects crumb rubber has on the mix. A comparison between our model and the experimental data can be seen in Figure 8, with TDA and Crumb rubber of 7.5% and 15%. Three cylinders were tested for each rubber content. As shown in Figure 8(a), the proposed equation agrees significantly with the Siringi's experimental results for concrete cylinders containing 7.5% TDA replacing the coarse aggregates, with minimal deviation observed. The average standard 28-day compressive strength of the ordinary concrete use to create the 7.5% TDA mixture had a compressive strength of 28 MPa and a strain at peak of 0.00166 mm/mm.

The proposed equation could be used to describe also the behaviour of crumb rubber replacing the fine aggregates by volume as well. As shown in Figure 8(b), there is a very small difference between the proposed equation and the specimen's stress-strain behaviour in the beginning of the loading phase, then the model overlaps the experimental results towards the second half of the loading phase up until failure for the 7.5% crumb rubber. Likewise, Siringi's experimental data for crumb rubber replacing 15% of the fine aggregate's volume is accurately depicted by the proposed model as seen in Figure 8(c). The ordinary concrete used to make the mix had an average standard 28-day compressive strength of 28 MPa and a strain at peak of 0.0013 mm/mm. Although the equation gives a slightly lower ultimate stress, the data overlaps the equation's curve up until the yielding point.

Similarly, Toutanji (1996) investigated the replacement of mineral coarse aggregate by rubber tire. Four different volume contents of rubber tire chips were used: 25, 50, 75 and 100%. The maximum coarse aggregate size was 19 mm, while the fine aggregate (sand) had a maimum size of 4.76 mm. The shredded tire particles used had a maximum size of 12.7 mm and were all graded within the limits of the ASTM C 33. Cylindrical specimens measuring 100 mm in diameter and 200 mm in height were prepared and tested under compression. The average 28-day compressive strength was 31.9 MPa and the strain at peak was 0.0019 mm/mm. the stress strain behaviour of the ordinary concrete prepared is compared with the results obtained from the proposed equation in Figure 9. The model accurately predicts the stress strain behaviour of the concrete mix containing 50% and 100% rubber aggregates replacing the coarse aggregates by volume, especially at R_C =100% as shown in Figure 8.

Gou et al. (2014) studied the compressive behaviour of ordinary concrete and recycled aggregate concrete under elevated temperatures and compared their stress strain behaviour. Fine

aggregates were naturally sourced medium-coarse rive sand. Coarse aggregates, obtained from limestone, had a maximum aggregate size of 12.5 mm. The recycled concrete coarse aggregates used were obtained from crushed waste concrete and ranged from 4.75 mm to 12.5 mm in size. The crumb rubber particles used ranged from 0.85 mm to 1.4 mm. cylindrical specimens measuring 150 mm by 300 mm were made using the given material, with crumb rubber replacing 4%-16% of the coarse aggregates by volume through 4% increments. The 28 day compressive strength of the ordinary concrete was 60 MPa and the strain at peak was 0.0027 mm/mm, while the 28 day compressive strength of the recycled aggregate concrete was 52 MPa and the strain at peak was 0.003 mm/mm. The specimens underwent compressive tests to investigate the effect crumb rubber has on the recycled aggregate concrete. The stress strain behaviour of these specimens can be seen in Figure 10. It is evident that the proposed model effectively anticipates the behaviour of the specimens with great accuracy and precision.

5. CONCLUSIONS

A total of 44 concrete cylinders (150 mm x 300 mm) were prepared and tested under compression in this study. The specimens had their coarse aggregates replaced by tire derived aggregates (TDA) by volume following a 10% increment starting from TDA-0 (ordinary concrete, which serve as the control specimens) up till TDA-100 (coarse aggregate comprised of TDA only). The specimens underwent compressive tests to reveal the variance of certain mechanical properties like compressive strength, strain and modulus of elasticity with a change in TDA content of the concrete specimen. A summary of these results can be seen in Table 3. It was observed that an increase in TDA content was followed by a decrease in strength but allowed for a less brittle failure. The specimens showed some visible deformation before experiencing failure, which served

as a warning. Hence, TDA content in concrete can be increased for applications where strength is not vital for the successful performance of the structure. Adding TDA to the concrete resulted in a more ductile post peak behaviour relative to the control ordinary concrete.

This allowed the concrete specimens to undergo greater deformations without the disintegration of the overall concrete specimen. Likewise, plastic energy absorption capacity increased with an increase in TDA, making TDA concrete useful for seismic and vibration applications where better damping and absorbing abilities are needed. Similarly, as TDA content increased the elastic modulus decreased. Equations describing these changes in mechanical properties of the concrete as TDA content changes have been developed. Such relations could be helpful in predicting the behaviour of concrete structures based on the TDA content within them. These models would make the application of rubberized concrete to the engineering field more practicial and useful, as it would give an enhanced design grasp on various design variables associated with the structure.

6. ACKNOWLEDGEMENTS

Authors would like to thank Koosha Khorramian, Jordan Maerz, Jesse Keane, and Dillon Betts for their assistance in the lab. The authors would also like to acknowledge and thank NSERC and Dalhousie University for their financial support.

7. REFERENCES

ASTM C33/C33M-13. 2013. Standard specification for concrete aggregates. ASTM International, West Conshohocken, PA, USA.

Bandarage, K., and Sadeghian P. 2019. Effects of long shredded rubber particles recycled from waste tires on mechanical properties of concrete. Journal of Sustainable Cement-Based Materials, In Press, DOI:10.1080/21650373.2019.1676839.

Bideci, Ö. S., Saka, R. C., and Bideci, A. 2017. Physical characteristics of rubberized concrete including granulated waste tire aggregate. *Politeknik Dergisi*, *20*(4), 777-786.

El Naggar, H., Soleimani, P., and Fakhroo, A. 2016. Strength and stiffness properties of green lightweight fill mixtures. Geotechnical and Geological Engineering, 34(3), 867-876.

El Naggar, H., Turan, A., and Hafez, D. 2013. Static and Seismic Behavior of Culverts Constructed with TDA Inclusion. 66th Canadian Geotechnical Conference, Montreal, Quebec, Canada.

Elchalakani, M. 2015. High strength rubberized concrete containing silica fume for the construction of sustainable road side barriers. Structure, 1, 20-38.

Eldin, N. N., and Senouci, A. B. 1992. Engineering properties of rubberized concrete. Canadian Journal of Civil Engineering, 19(5), 912-923.

Eldin, N. N., and Senouci, A. B. 1994. Measurement and prediction of the strength of rubberized concrete. Cement and Concrete Composites, 16(4), 287-298.

Ghaly, A. M., and Cahill IV, J. D.(200). Correlation of strength, rubber content, and water to cement ratio in rubberized concrete. Canadian Journal of Civil Engineering, 32(6), 1075-1081.

Gholampour, A., Ozbakkaloglu, T., and Hassanli, R. 2017. Behavior of rubberized concrete under active confinement. Construction and Building Materials, 138, 372-382.

Guo, Y. C., Zhang, J. H., Chen, G. M., and Xie, Z. H. 2014. Compressive behaviour of concrete structures incorporating recycled concrete aggregates, rubber crumb and reinforced with steel fibre, subjected to elevated temperatures. Journal of cleaner production, 72, 193-203.

Hognestad, E. 1951. *A study on combined bending and axialload in reinforced concrete members*.

Champaign, IL:University of Illinois at Urbana-Champaign.

Jafarian Abyaneh, M., Sadeghian, P., and El Naggar, H. 2018. Tire-Derived Aggregate Concrete for Bridge Applications. In 10th International Conference on Short and Medium Span Bridges (SMSB), Quebec City, QC, Canada. Canadian Society for Civil Engineering.

Khaloo, A. R., Dehestani, M., and Rahmatabadi, P. 2008. Mechanical properties of concrete containing a high volume of tire–rubber particles. Waste management, 28(12), 2472-2482.

Li, D., Zhuge, Y., Gravina, R., and Mills, J. E. 2018. Compressive stress strain behavior of crumb rubber concrete (CRC) and application in reinforced CRC slab. Construction and Building Materials, 166, 745-759.

Li, J., Saberian, M., and Nguyen, B. T. 2018. Effect of crumb rubber on the mechanical properties of crushed recycled pavement materials. Journal of environmental management, 218, 291-299.

Liu, F., Meng, L. Y., Chen, G. X., and Li, L. J. 2015. Dynamic mechanical behaviour of recycled crumb rubber concrete materials subjected to repeated impact. Materials Research Innovations, 19(sup8), S8-496.

Liu, B., Yang, S., Li, W., & Zhang, M. 2020. Damping dissipation properties of rubberized concrete and its application in anti-collision of bridge piers. *Construction and Building Materials*, *236*, 117286.

Mahgoub A., and El Naggar, H. 2020a. Innovative Application of Tire-Derived Aggregate around Corrugated Steel Plate Culverts. Journal of Pipeline Systems Engineering and Practice, 10.1061/(ASCE)PS.1949-1204.0000466

Mahgoub A., and El Naggar, H. 2020b. Coupled TDA-Geocell Stress-Bridging System for Buried Corrugated Metal Pipes. Journal of Geotechnical and Geoenvironmental Engineering 146 (7). DOI: 10.1061/(ASCE)GT.1943-5606.0002279

Mahgoub, A., and El Naggar, H. 2019. Using TDA as an Engineered Stress-Reduction Fill over Preexisting Buried Pipes. Journal of Pipeline Systems Engineering and Practice, 10(1), 04018034.

Miller, N. M., and Tehrani, F. M. 2017. Mechanical properties of rubberized lightweight aggregate concrete. Construction and Building Materials, 147, 264-271.

Najim, K. B., and Hall, M. R. 2012. Mechanical and dynamic properties of self-compacting crumb rubber modified concrete. Construction and building materials, 27(1), 521-530.

Ozbay, E., Lachemi, M., and Sevim, U. K. 2011. Compressive strength, abrasion resistance and energy absorption capacity of rubberized concretes with and without slag. Materials and structures, 44(7), 1297-1307.

Pham, T. M., Elchalakani, M., Hao, H., Lai, J., Ameduri, S., and Tran, T. M. 2019. Durability characteristics of lightweight rubberized concrete. *Construction and Building Materials*, *224*, 584-599.

Siddiqi, Z., Hameed, R., and Akmal, U. "Permeability and Strength Properties of Rubberized Concrete". Project Report, ASTM International, West Conshohocken, PA, USA. https://www.astm.org/studentmember/images/Study-of-the-Permeability-of-Rubberized-Concrete.pdf

Siringi, G. M. 2012. Properties of Concrete with Tire Derived Aggregate and Crumb Rubber as a Ligthweight Substitute for Mineral Aggregates in the Concrete Mix. PhD Dissertation, University of Texas Arlington, Arlington, TX, USA.

Siringi, G., Abolmaali, A., and Aswath, P. 2015. Properties of Concrete with Tire Derived Aggregate Partially Replacing Coarse Aggregates. The Scientific World Journal, 2015, 13.

Sparkes, J., El Naggar, H., and Valsangkar, A. 2019. Compressibility and shear strength properties of tire derived aggregate mixed with lightweight aggregate. Journal Of Pipeline Systems, ASCE. 10(1), 04018031.

Toutanji, H. 1996. The use of rubber tire particles in concrete to replace mineral aggregates. Cement and Concrete Composites, 18(2), 135-139.

Wong, S. F., and Ting, S. K. 2009. Use of recycled rubber tires in normal-and high-strength concretes. ACI Materials Journal, 106(4), 325.

Xue, J., and Shinozuka, M. 2013. Rubberized concrete: A green structural material with enhanced energy-dissipation capability. Construction and Building Materials, 42, 196-204.

Zahran, K., and El Naggar, H. 2020. Effect of Sample Size on TDA Shear Strength Parameters in Direct Shear Tests. Transportation Research Record. (In press)

Zheng, L., Huo, X. S., and Yuan, Y. 2008. Strength, modulus of elasticity, and brittleness index of rubberized concrete. Journal of Materials in Civil Engineering, 20(11), 692-699.

Table 1: Test matrix

Specimen ID	TDA content (%)	Number of specimens	Coarse Aggregate (kg/m^3)	Fine Aggregate (kg/m^3)	TDA (kg/m^3)
TDA-0	0	4	958	559	0
TDA-10	10	4	862	559	33
TDA-20	20	4	767	559	67
TDA-30	30	4	671	559	100
TDA-40	40	4	575	559	133
TDA-50	50	4	479	559	167
TDA-60	60	4	383	559	200
TDA-70	70	4	287	559	233
TDA-80	80	4	192	559	267
TDA-90	90	4	96	559	300
TDA-100	100	4	0	559	333

* Each specimen was prepared with 657 kg/m^3 cement, 221 kg/m^3 water (i.e., water to cement ratio, W/C=0.33)

Table 2: Material properties

Material	Type	Sample Size (kg)	Maximum Aggregate Size (mm)	Minimum Aggregate Size (mm)	Bulk Densities (kg/m³)
Cement	Portland Type 1	---	---	---	---
Coarse Aggregate	12 mm Gravel	6	19.05	4.75	1601
Fine Aggregate	Saturated Surface Dry (SSD) Masonry Sand	2	9.50	0.15	1817
TDA	Shredded Tires	8	25.40	4.75	557

Table 3: Summarized specimens' mechanical properties

TDA Content (%)	Density (kg/m^3)		Compressive Strength			Elastic Modulus			Strain at Peak (%)	
	Average Value	SD	Average Value (MPa)	Specific Strength (kN·m/kg)	SD (MPa)	Average Value (Gpa)	Specific Elastic Modulus (10^6 N.m/kg)	SD (GPa)	Average Value	SD
0	2552	3	65.7	25.8	2.0	39.2	15.4	0.6	0.205%	0.019%
10	2473	5	46.9	19.0	0.6	36.0	14.6	0.7	0.228%	0.008%
20	2433	11	43.7	17.9	0.9	35.0	14.4	0.9	0.258%	0.005%
30	2374	6	42.0	17.7	0.9	32.4	13.7	1.3	0.281%	0.007%
40	2321	15	38.2	16.5	1.6	28.5	12.3	1.5	0.290%	0.014%
50	2263	27	29.9	13.2	1.4	24.1	10.7	1.4	0.319%	0.014%
60	2213	25	26.1	11.8	0.7	21.6	9.8	1.8	0.336%	0.007%
70	2180	16	24.2	11.1	1.1	18.7	8.6	0.3	0.364%	0.005%
80	2118	26	20.6	9.8	1.3	17.2	8.1	0.6	0.376%	0.005%
90	2048	44	17.7	8.7	0.9	14.7	7.2	0.7	0.387%	0.005%
100	2014	3	14.4	7.1	1.5	11.8	5.8	1.7	0.391%	0.006%

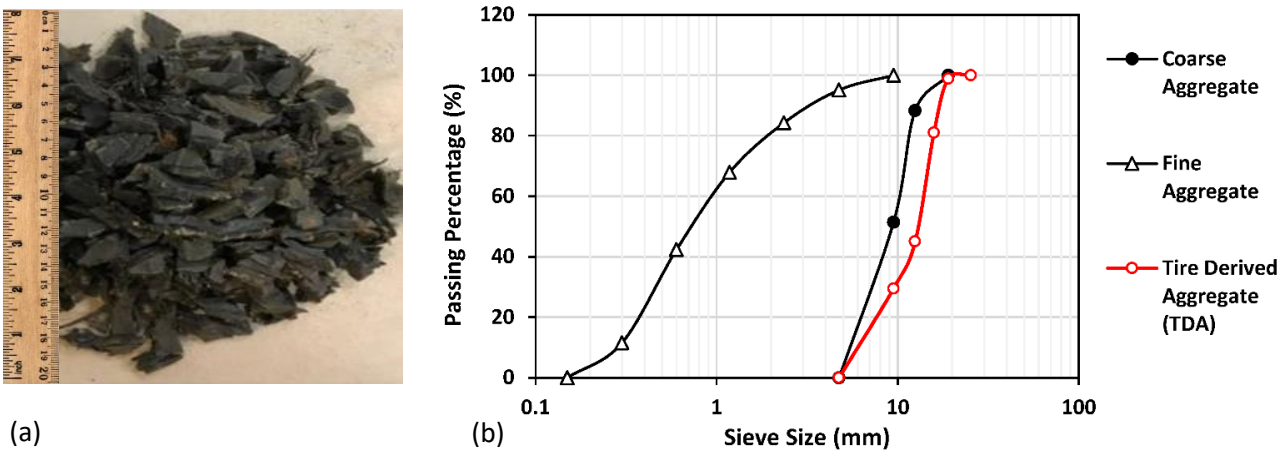

Figure 1: a) sample of the used TDA, b) gradation curves of the used materials

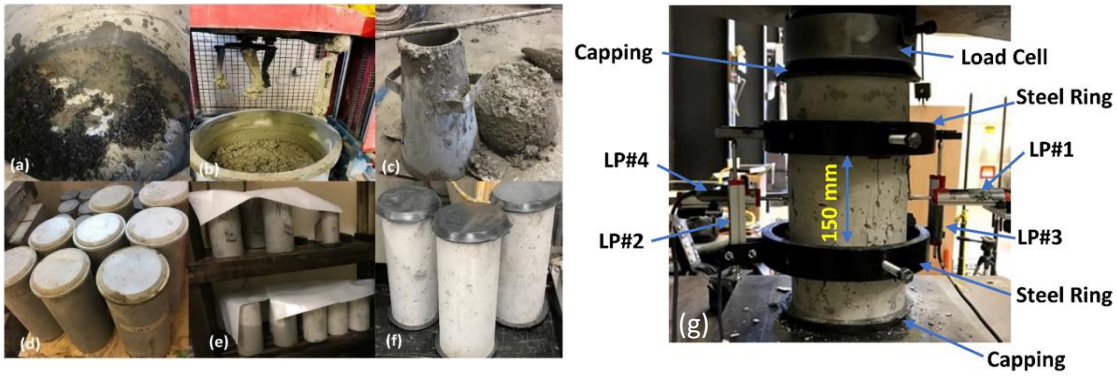

Figure 2: Specimen preparation: (a) concrete material placed in the concrete mixer, (b) mixing concrete material (c) conducting slump test to ensure 100 mm slump is attained, (d) Placing concrete in cylindrical molds for 24 hours, (e) placing specimens in curing room for 28 days, and (f) capping the specimens, (g) test setup and instrumentation.

Figure 3: Cylindrical concrete specimens after failure

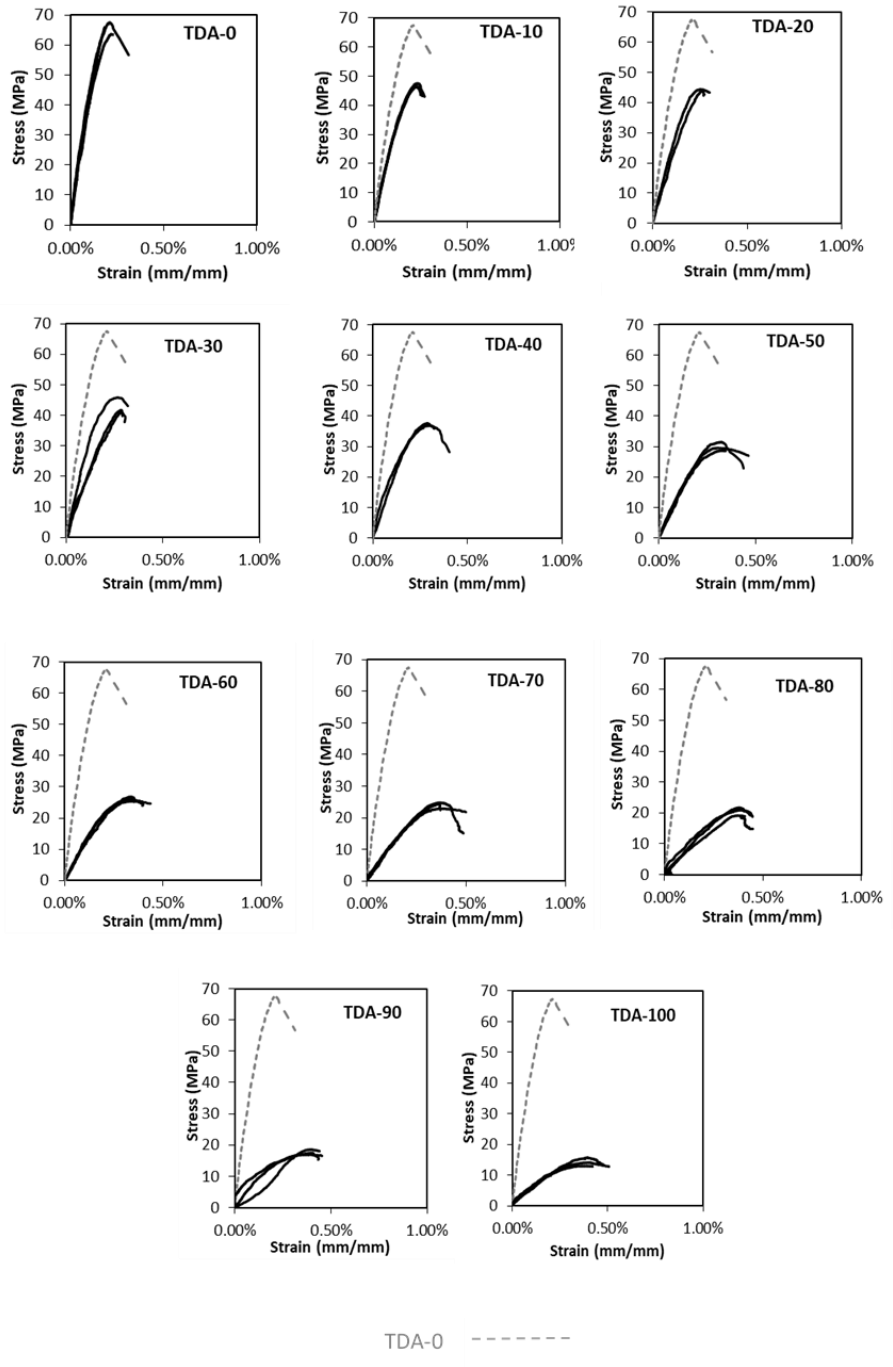

Figure 4: Stress-strain curves at each TDA increment

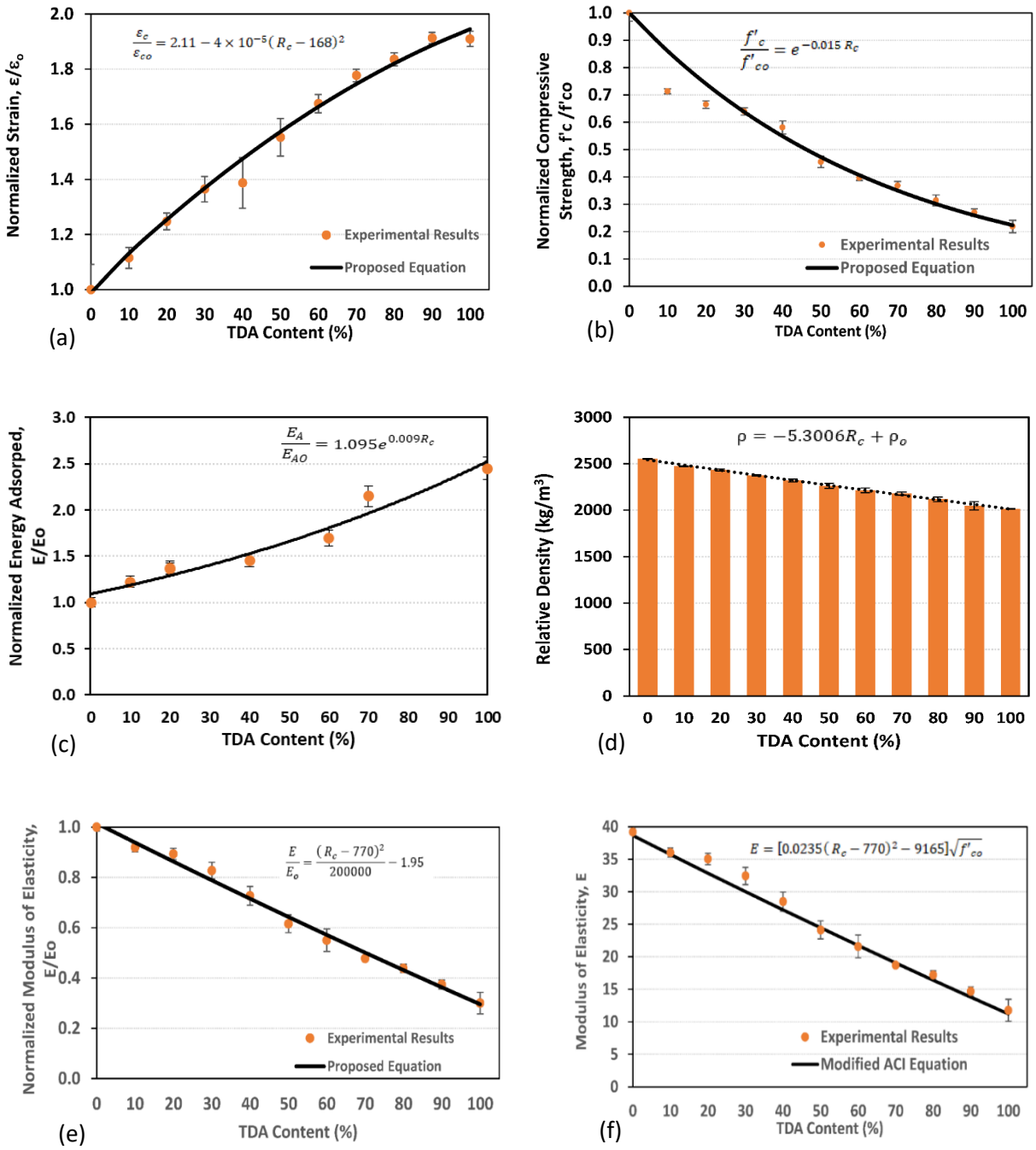

Figure 5: a) normalized strain vs TDA content, b) normalized compressive strength vs. TDA content, c) normalized energy adsorped by the concrete specimens vs. TDA content, d) relative density of the concrete specimens vs. TDA content, e) normalized modulus of elasticity vs. TDA content, f) experimentally obtained elastic modulus values plotted along with the modified model values.

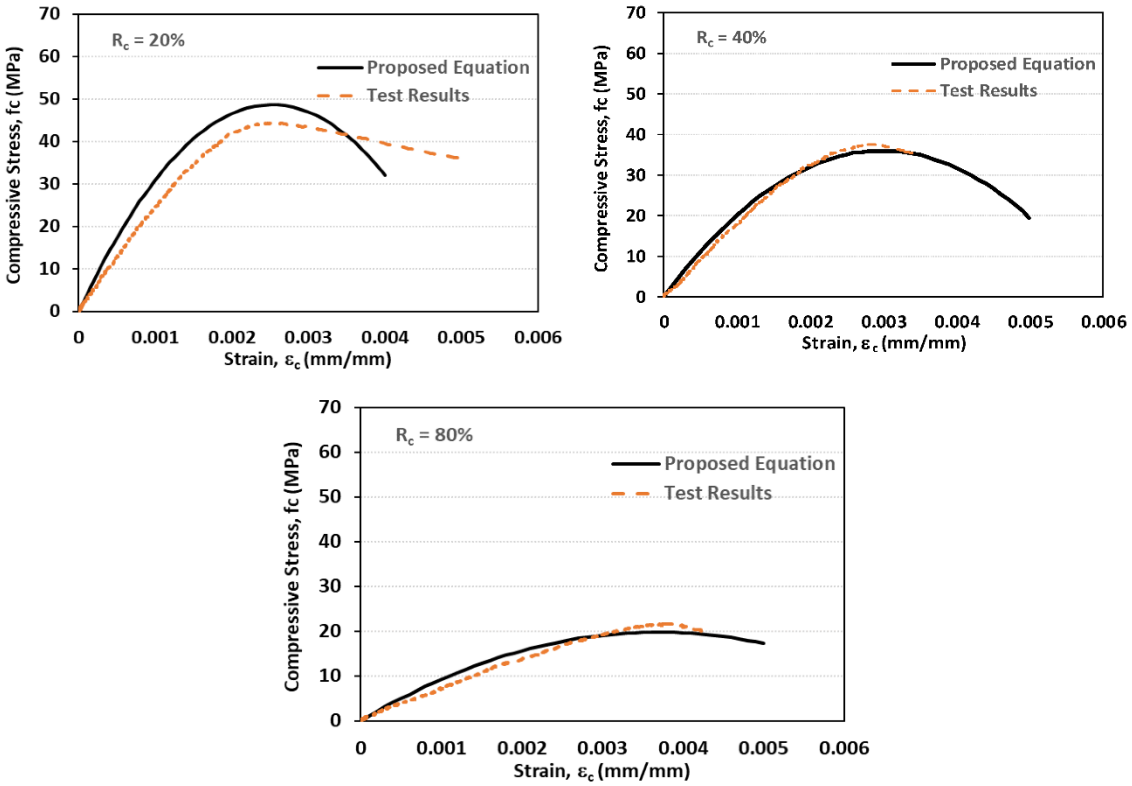

Figure 6: Comparison between test results (current study) and the proposed equation

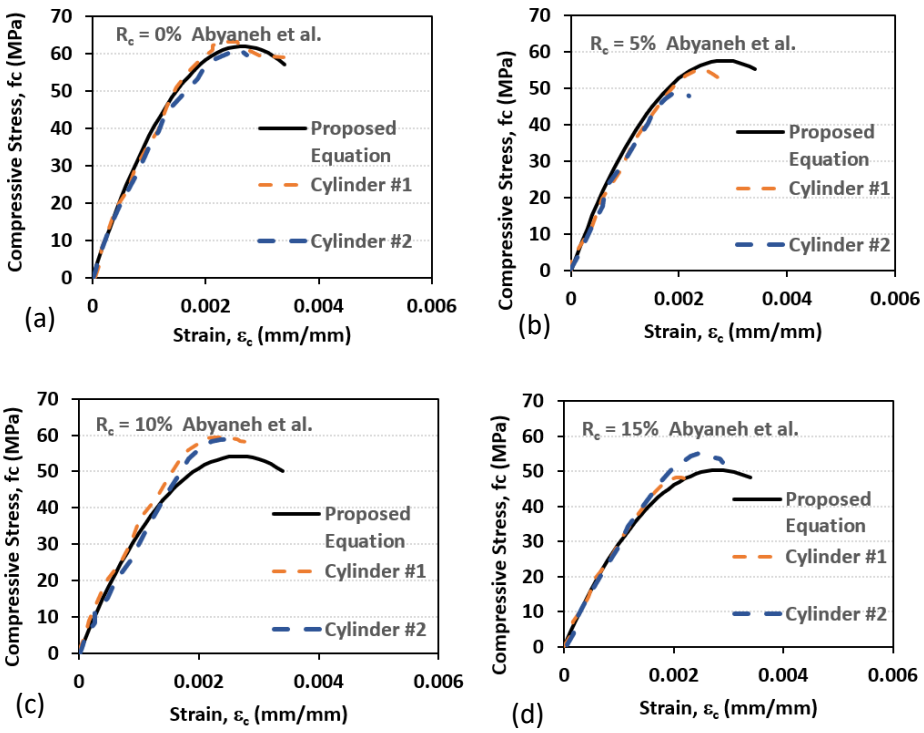

Figure 7: Performance of the proposed stress-strain model against test data by Abyeneh et al. (2018): (a) 0% TDA, (b) 5% TDA, (c) 10% TDA, and (d)15% TDA

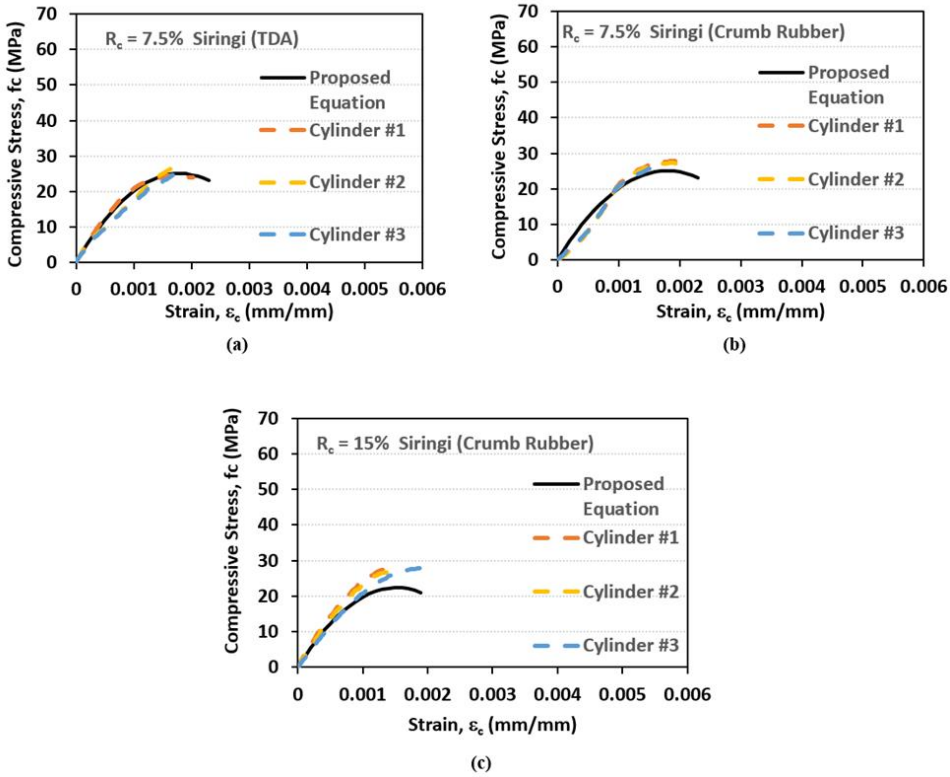

Figure 8: Performance of the proposed stress-strain model against test data by Siringi (2012): (a) 7.5% TDA, (b) 7.5% Crumb Rubber, and (c) 15% Crumb Rubber

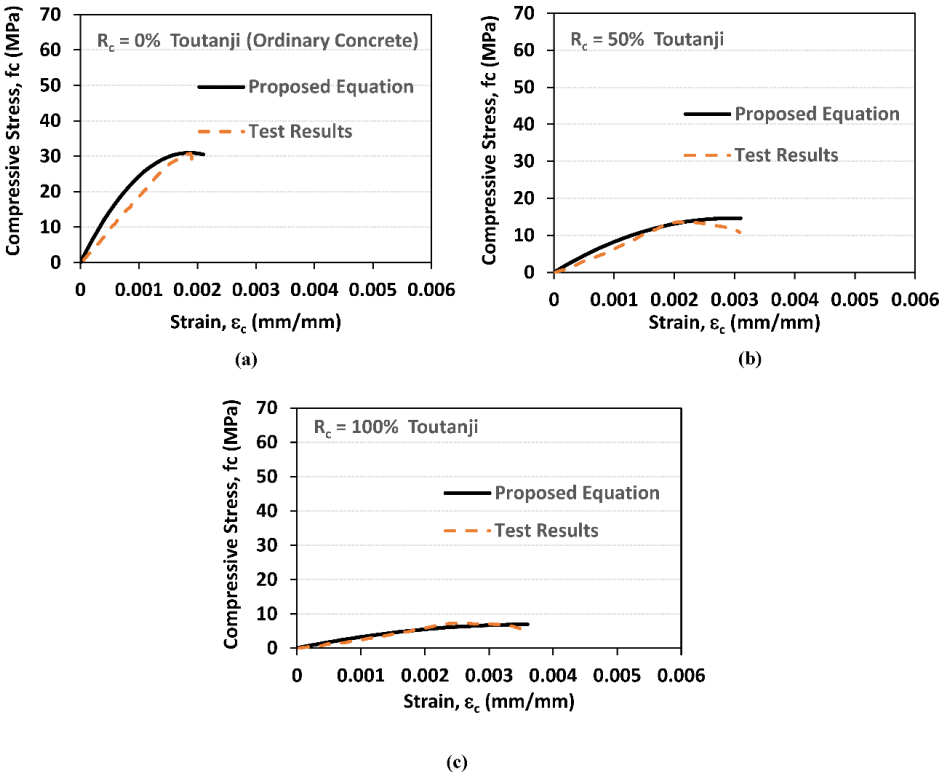

Figure 9: Performance of the proposed stress-strain model against test data by Toutanji (1996): (a) 0% TDA, (b) 50% TDA, and (c) 100% TDA

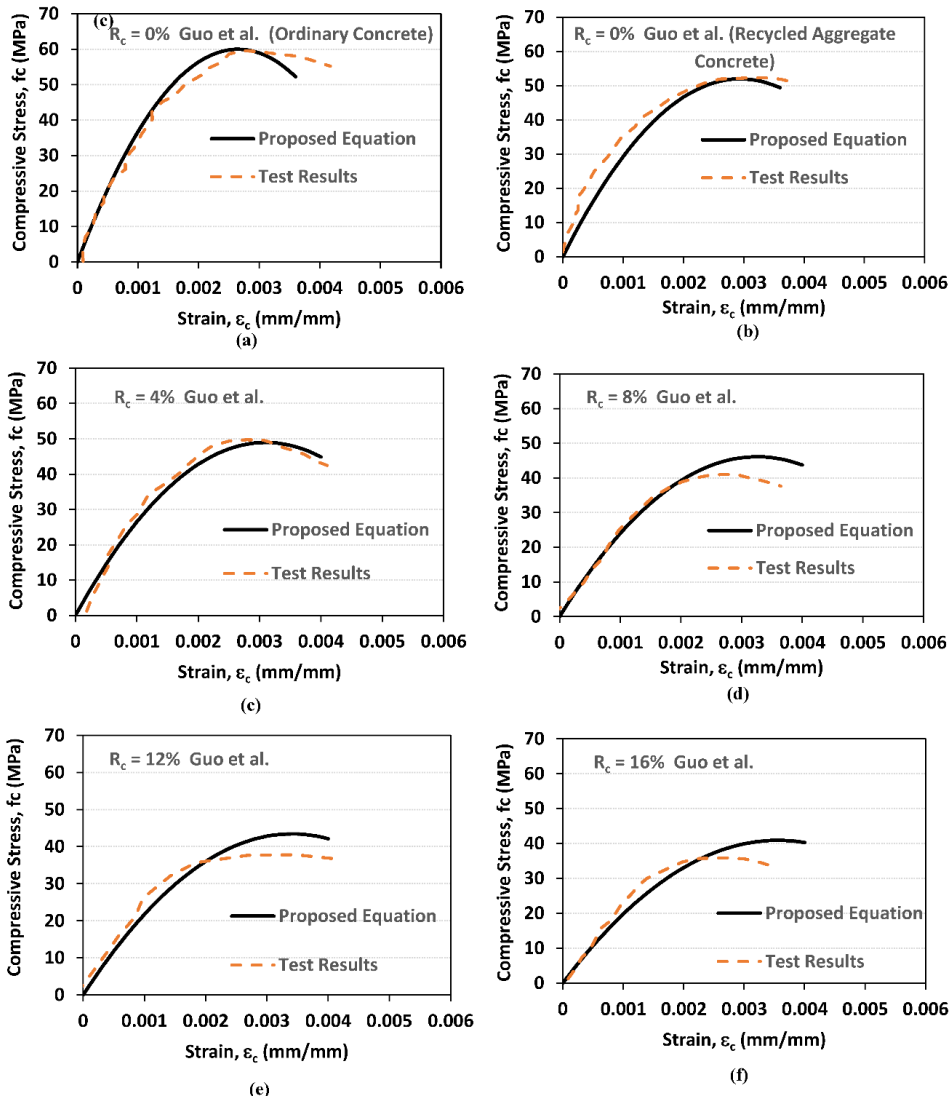

Figure 10: Performance of the proposed stress-strain model against test data by Gou et al. (2014): (a) 0% TDA (ordinary concrete), (b) 0% TDA (recycled aggregate concrete), (c) 4% TDA, (d) 8% TDA, (e) 12% TDA, and (f) 16% TDA